TEM

EDS in the TEM Explained

OXFORD INSTRUMENTS

The Business of Science®

1.0 Introduction

Modern transmission electron microscopes (TEM) can be regarded as complex analytical tools that provide information about the structure, crystallography and chemistry of materials. They may be basic instruments with a thermionic electron source that can provide limited information such as bright-field and dark-field imaging for visual interpretation of structures and selected area diffraction (SAED) for crystallographic information. At the other end of the range, there are cold field-emission source (CFEG) instruments with aberration correctors that enable the study of structures on atomic scale with an array of available techniques including atomic level imaging, using TEM and scanning transmission electron microscopy (STEM) nano-diffraction, energy loss spectroscopy (EELS) and energy dispersive spectroscopy (EDS). For most applications in materials science, a minimum of 200 kV accelerating voltage is required for sample penetration and analytical capability in the form of EDS and possibly EELS. Aberration Corrected TEMs are capable of atomic column elemental mapping and picometer level imaging, and will be discussed later in this technical briefing.

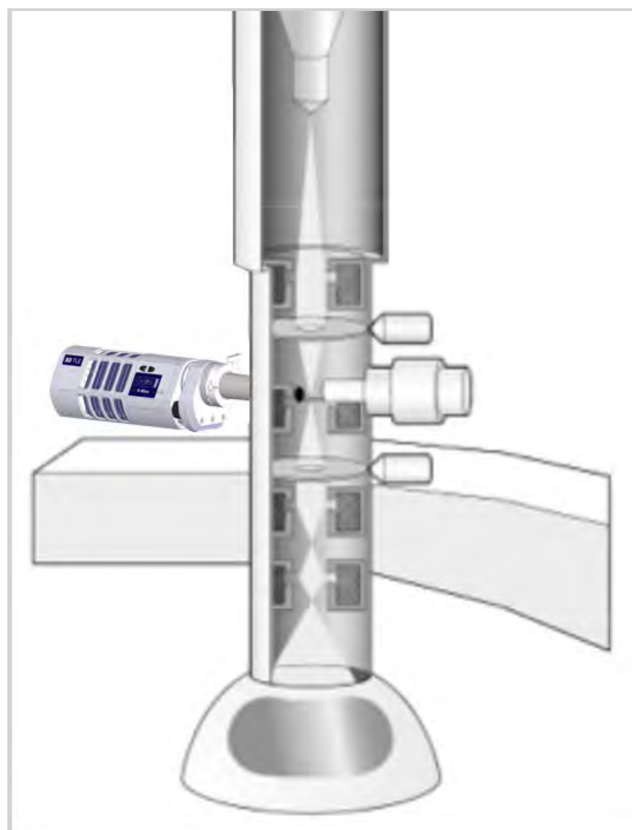

Fig. 1. *TEM cross-section showing lenses and sample position.*

2.0 Fundamentals of TEM technique

In TEM, just as in light microscopy, a beam is passed through a series of lenses (Figure 1) to form a magnified image of a specimen in the area of the objective lens (Figure 1a). This image may then be viewed on a fluorescent screen or CCD camera. Unlike a light microscope, the TEM operates under vacuum because electrons are easily scattered at atmospheric pressure. The lenses are electromagnetic as opposed to glass which is opaque to electrons. Electromagnetic lenses have the advantage that the magnification, focus and beam diameter may be easily changed by adjusting lens currents. However, these lenses are subject to aberrations, which must be corrected electronically. This can be accomplished by basic stigmation correction or more sophisticated aberration correctors to remove spherical (Cs) and chromatic (Cc) aberration from the condenser and objective lenses. Due to the complexity of contemporary analytical TEMs most processes are computer controlled for ease of use as there are many variable parameters depending upon the imaging and or analytical techniques being used. Note that whereas the light microscope has a resolution limit in the order of 100 nm, modern TEMs are now capable of atomic imaging in the picometer range.

Early in the development of TEM, it was discovered that materials diffract electrons and that if this material is crystalline a diffraction pattern is formed in the back focal plane of the objective lens. This image can be recorded on film or CCD camera to give valuable information on the structural and crystallographic nature of materials under investigation. It was also found that if the beam could be formed into a fine probe, other signals could be generated from very small regions of the specimen, so chemistry and structure could be determined from these regions. In addition, if scan coils are fitted to the optical column, this focused beam could be scanned across the sample in the same way as in the SEM but in this case a scanning transmission (STEM) image may be formed. Various bright-field and dark-field STEM images may be collected in this way. It is also possible to create X-ray maps of materials by using a suitably placed X-ray detector in the microscope

column. TEMs have been equipped with spectrometers to detect X-rays since the late 1960s. The first dedicated analytical TEM was the Electron Microscope Micro-Analyzer (or EMMA) developed by AEI. This was unique in that primary analysis was performed by Wavelength Dispersive Spectrometry (WDS) rather than EDS. Although WD spectrometers have better spectral resolution than EDS, collection efficiency is poor, and spectrometer stability was a problem with this instrument. EDS was first used on TEMs in the early 1970s, and provided much better collection efficiency along with the ability to collect a range of elements from Na to U simultaneously. This, with the ability to produce high-energy probes with a spatial resolution on the nanometer range, created the first truly viable analytical TEMs.

3.0 Beam-specimen interaction in the TEM

Although similar in many ways to EDS analysis in the SEM, there are marked differences when analysing TEM samples. In general, SEM samples are thick enough for a focused probe to be contained within the sample, i.e. there is no transmission of the primary beam because it cannot pass all the way through the sample. This causes the beam to scatter within the sample, and a number of factors need to be considered when treating the raw X-ray data for quantitative analysis. These include atomic number (Z), X-ray absorption (A) and fluorescence (F), which are dealt with by applying matrix corrections. The incident beam energy, sample density and take-off angle, therefore have a profound effect on quantitative results in the SEM.

However, this is not the case with TEM as samples should be beam transparent, usually in the order of 100 nm or less, and beam energies are generally much higher and therefore have more penetrating power. As can be seen in Figure 2, the ionization volume in the path of the focused probe is much smaller than it would be in the SEM. Consequently spatial resolution is far better because there is far less scattering of the primary beam by the sample.

Due to the fact that the irradiated volume is much smaller than that in the SEM count rates tend to be lower. However, if samples are thicker than 100 nm, results may need to be corrected for density and absorption.

The other signals in the above diagram are complementary to the X-ray signal and offer other types of chemical and structural data on the sample. Many of these signals can be obtained simultaneously under the same conditions e.g. nano-diffraction patterns and Energy Loss Spectroscopy (EELS) spectra, so a large amount of information can be made available without having to change the microscope conditions or move the sample.

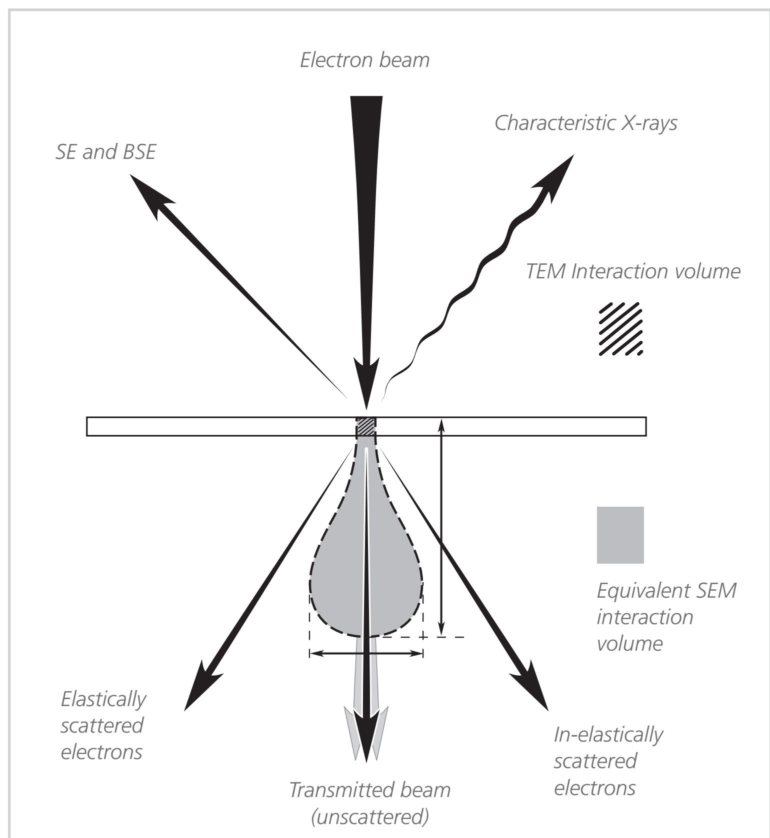

Fig. 2. *Electron beam/sample interaction.*

4.0 The Analytical TEM (ATEM

As stated above, analytical TEMs are usually equipped with a variety of detectors including both backscattered, bright-field and dark-field STEM detectors. These detectors not only aid in imaging but also may reveal the chemical composition of the specimen itself. EELS is also very sensitive to lighter elements, and is an excellent auxiliary tool to EDS, especially as EELS can sometimes give bonding information that is not available using EDS. However, EDS remains the analytical method of choice in many cases due to its ease of use, ability to analyse elements across the periodic table and relatively simple interpretation.

Due to the confined space around the polepiece and specimen, correct placing and collimation of the X-ray detector is vitally important. State-of-the-art, high-resolution TEMs have polepiece gaps of a few millimeters, and it is necessary to get the detector as close as possible to increase solid angle (or collection efficiency), while making sure that the detector does not detect stray elemental peaks due to incorrect positioning. The electron column must also be designed to minimize stray radiation in the form of hard X-rays passing down the column. These hard X-rays, if not checked, can generate characteristic X-rays from the polepiece area and the sample holder. They may also cause X-ray generation from parts of the grid other than the area being analysed. Analytical TEMs are therefore equipped with special apertures to eliminate hard X-rays passing down the column and generating spurious peaks from the polepiece and other regions in the sample area.

A number of tests are commonly performed to assess the "cleanliness" of an electron column. These include the hole count, which determines the amount of stray X-rays being generated by the TEM. This can be calculated using a NiO_x film on a carbon support mounted on a Mo grid. These grids (see Figure 3). are available from microscope accessory suppliers. The hole-count ratio can be represented by the following formula:-

HCR = [T(Ni) – B(Ni)] / [T(Mo Kα) – B(Mo Kα)]hole

Where T = total counts in an energy window over the elemental peak, and B = the background on either side of these peaks.

Here the Ni Ka peak from the film is divided by the Mo Kα peak measured in a nearby grid square containing no film. The contribution from the Mo grid is not generated by scatter from the NiO_x specimen, and therefore represents Mo X-rays generated by electrons that are backscattered from the polepiece and/or hard X-rays.

Another common test of microscope performance is the peak-to-background ratio, and is defined as the total number of characteristic counts in a particular peak divided the background counts under that peak. If the background is integrated over 600 eV, the peak/background ratio at the Ni peak is:-

P/B10 = 60[T(Ni Kα) – B(Ni Kα)] / [B(Ni Kα)]

For current 200 – 300 kV analytical TEM, this value should be in the region of 4000. Low values of P/B10 may result from stray column radiation, generating Bremsstrahlung in thick regions of the sample, the specimen holder or from EDS system electronics or ground loops.

Detector geometry for TEM presents a special challenge for designers due to the limited space of the polepiece area where the sample resides (see Figure 4). Ideally, the detector should be able to view the X-rays from above the specimen so that the sample can be analysed in a horizontal or nearly horizontal position.

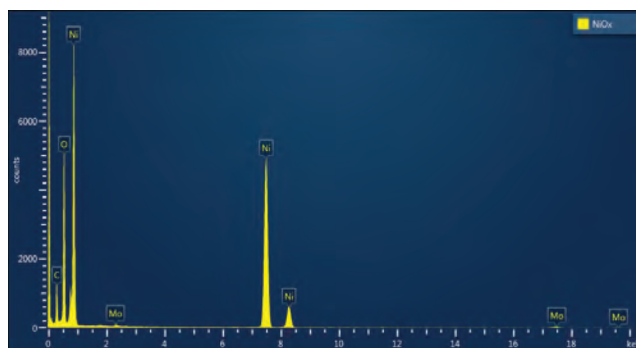

Fig. 3. *Typical NiOx spectrum.*

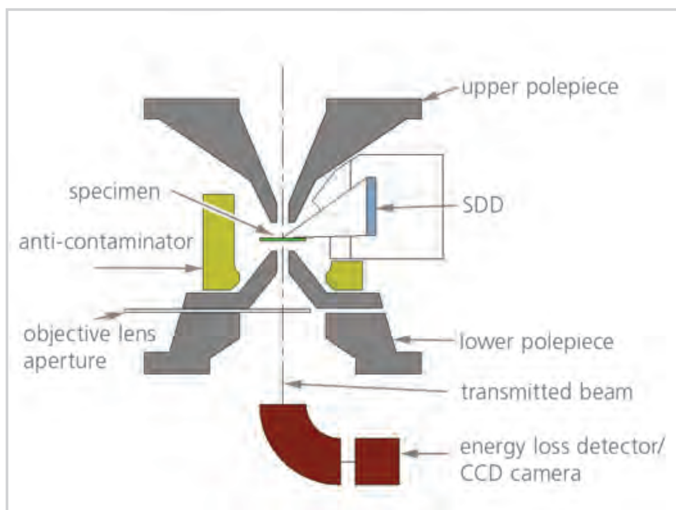

Fig. 4. *Objective lens polepiece cross section.*

The positioning of the detector in relation to the sample can be defined by the sample-to-sensor distance or the collection angle, and the take-off angle (TOA) relative to the horizontal specimen plane (see Figure 5).

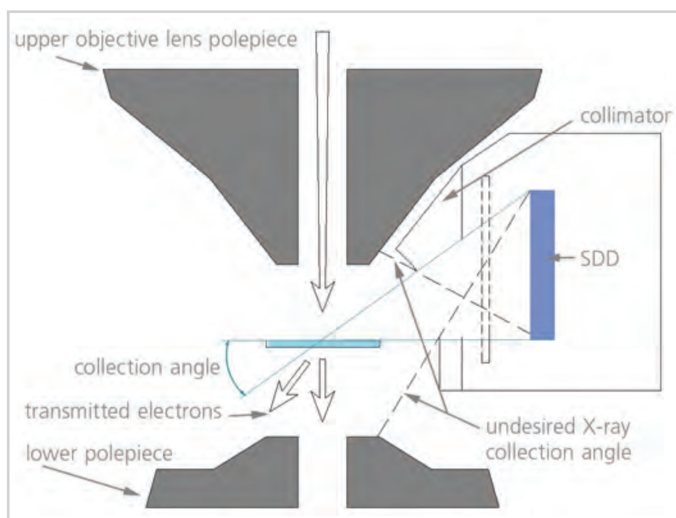

Fig.5. *Detector polepiece geometry (after Williams and Carter, 1996).*

Care should be taken to limit the entry of backscattered electrons into the detector because magnetic electron traps (as employed in SEM columns) cannot be used in TEMs as the the detector is close to the electron beam in the objective lens area. This would cause aberrations such as astigmatism in the beam and limit the performance of the TEM. Consequently, collimator design is very important. The detector solid angle is a function of the detector area, polepiece and collimator design, and is an important factor in characteristic X-ray detection. Although solid angle may be increased by placing the detector close to the sample, care should be taken that the collimator design is adequate to eliminate the effects of backscattered electrons and spurious X-rays. Very often, the placement of the detector is limited by the design of the TEM polepiece. Larger area detectors are now available for TEMs which also tend to increase solid angle, and these will be discussed later.

Solid angles of TEMs are generally in the order of 0.1 – 0.5 steradians although values of up 1.0 steradians have been reported on specialised analytical tools. Although these solid angles are generally an order of magnitude higher than those experienced in an SEM, it must be remembered the volume being analysed in a TEM is far smaller, and hence the characteristic X-rays generated will be far less, so in most cases large solid angles are a prerequisite for TEMs. This is especially important for those TEMs using thermionic emitters such as a tungsten filament or LaB_6 filament where beam current density is low. Solid angle is also important when performing atomic-level analysis on field-emission source, aberration-corrected TEMs where beam current density is high but the amount of material under the probe is extremely small.

There are a number of different detector front-end designs, including those with polymer windows, support grids, and there are also windowless detector models. Consequently it is unwise to use a simple geometric formula (e.g. A/d^2) based on the area of the detector (A) and the distance (d) of the sensor from the sample. This is especially the case for detectors that are not circular. Solid angle may also be measured by comparing counts collected from well categorised materials at given beam currents. However, no standard method has been adopted by the various TEM manufacturers, and this area needs a more coordinated approach.

5.0 Detector design

5.1 Si(Li) detectors

The Si(Li) detector converts the energy of each X-ray into a voltage signal of proportionate size. This is achieved through a three-stage process:

1. The X-ray is converted into a charge by the ionization of atoms in a semiconductor crystal. (Figure 6a)
2. This charge is converted into the voltage signal by the FET preamplifier. (Figure 6b)
3. The voltage signal is input into the pulse processor for measurement. (Figure 6c.)

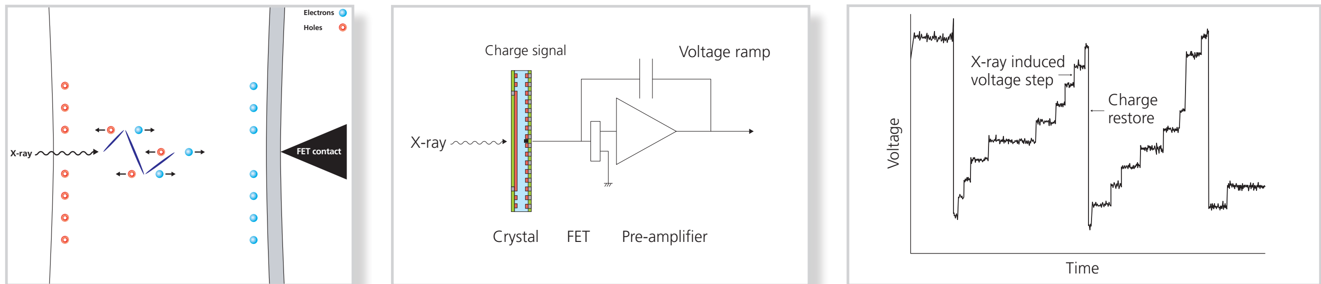

***Fig.** 6a, 6b, and 6c.*

When an incident X-ray strikes the detector crystal, its energy is absorbed by a series of ionizations within the semiconductor to create a number of electron-hole pairs (Figure 6a). The electrons are raised into the conduction band of the semiconductor, and are free to move within the crystal lattice. When an electron is moved to the conduction band, it leaves behind a "hole", which behaves like a free positive charge within the crystal. A high bias voltage applied between electrical contacts on the front face and back of the crystal then sweeps the electrons and holes to these opposite electrodes, producing a charge signal, the size of which is proportional to the energy of the incident X-ray. The charge is converted to a voltage by the FET preamplifier (Figure 6b). There are two sources of charge, current leakage from the crystal caused by the bias voltage between its faces, and the X-ray induced charge that is to be measured. The output from the FET caused by the charge build-up is a steadily increasing voltage 'ramp' due to leakage current, onto which is superimposed sharp steps due to the charge created by each X-ray event (Figure 6c). The accumulating charge has to be periodically restored to prevent saturation of the detector by using direct injection of charge into a specially designed FET. The noise is strongly influenced by the FET, and noise determines the resolution of the detector at low energies. Low noise is required to distinguish light elements such as beryllium from noise fluctuations. However, the charge signals generated by the detector are small and can only be separated from the electronic noise of the detector by cooling the crystal and FET to liquid-nitrogen temperatures. This is an obvious disadvantage because safety must be considered, and if the LN_2 supply is interrupted, it is not possible to use the detector. In addition, a Si(Li) detector is count rate limited due to the large size of its anode which results in high capacitance and voltage noise. This can cause the detector to saturate at high count rates, and this is especially problematic in TEM where high count rates may be generated when crossing sample grid bars or thicker areas of the specimen. In such cases, it is necessary to protect the detector by using a shutter or a fast retraction method. Either method tends to decrease productivity.

5.2 Silicon Drift Detectors (SDD)

In the last few years, new EDS detectors have emerged that do not require liquid nitrogen to cool them. These semiconductor devices, known as silicon drift detectors (or SDDs) were first manufactured in the 1980s for radiation physics. However, recent advances in fabrication methods have meant that they have been developed to become a viable alternative to Si(Li) detectors in a number of SEM EDS applications. In addition, new large-area EDS SDDs have emerged, which offer even greater benefits for micro- and nano-analysis. They combine for the first time, the potential for fast analysis and high productivity with operation at low beam currents.

The silicon drift detector (SDD) is fabricated from high-purity silicon with a large area contact on the entrance side. On the opposite side is a central small anode contact, which is surrounded by a number of concentric drift electrodes. When a bias is applied to the SDD detector chip and the detector is exposed to X-rays, it converts each X-ray detected to an electron cloud with a charge that is proportional to the characteristic energy of that X-ray. These electrons are then "drifted" down a field gradient applied between the drift rings and are collected at the anode.

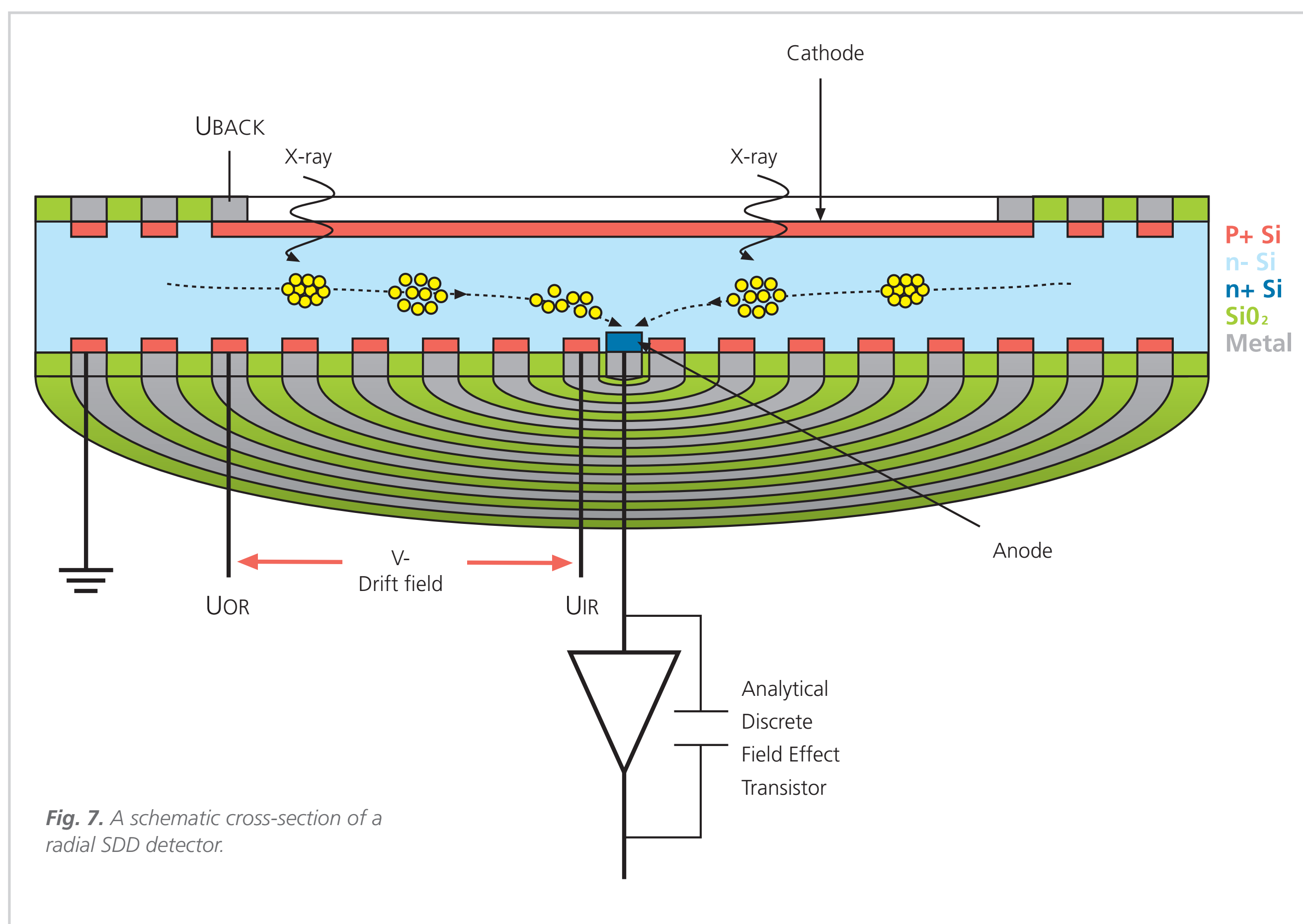

***Fig. 7.** A schematic cross-section of a radial SDD detector.*

Unlike a Si(Li) detector, however, the size of the anode on an SDD is small in comparison with the entrance contact. This results in lower capacitance and lower voltage noise. Therefore, short time constants can be used to minimize the effect of leakage current so that higher temperature Peltier cooling can be used instead of LN_2. This also means excellent resolution is achieved even at short process/shaping times and at count rates much higher than conventional Si(Li) detectors.

This gives distinct advantages when applied to the TEM in that the safety issues regarding LN_2 are eliminated, and the ability to tolerate high count rates in the order of ~ 500,000 cps allows moving over grids, bars etc. without saturating the detector. Also,

large-area sensors facilitate larger solid angles than Si(Li) detectors, which are limited to 50 mm² diameter if reasonable resolution is to be retained. SDDs have better resolution than Si(Li)s, especially at higher count rates, and low-energy X-rays show peak resolutions that are largely unattainable with Si(Li) detectors. In only a few years, SDDs have become the detector of choice for most TEM users and have superseded Si(Li) in all applications. Even SDDs need to be protected from high electron flux so in situations such as low-magnification mode, the detector is automatically retracted to increase its lifetime.

6.0 Analysis in the Transmission Electron Microscope (AEM)

6.1 Qualitative Analysis in the AEM

Many analytical observations in the AEM are qualitative. Often, it is only necessary to distinguish between phases, and it is not necessary to calculate elemental concentrations. Spectra may be collected at up to a 0 - 40 keV range as this aids in the identification of K lines of elements that may have overlapping L or M peaks in a lower range e.g. Pb and Mo. It is easier to detect small peaks from minor elements when the background is low. Counting for longer periods of time increases total counts, which reduces statistical scatter in the background. Increased counts can also be achieved by increasing probe current or analysing thicker parts of the specimen, although this involves some sacrifice in spatial resolution. Peak visibility is improved by having good detector resolution, which improves peak to background. To avoid false identifications, spurious peaks need to be eliminated by good collimation and the design of the sample holder. The limit of detection for an element, expressed as the minimum mass fraction (MMF), depends on the other elements present in the sample, microscope kV, detector resolution and the number of counts recorded in the spectrum. The MMF is usually calculated as the largest concentration that could be attributed to statistical fluctuations alone. By reducing statistical fluctuations, the MMF is improved. In a TEM, the total volume of material analysed is determined by the probe diameter and the specimen thickness. Therefore the total mass of material excited by the probe can be very small, and masses as small as 10^{-19}g or less can be measured with EDS.

Quantitative Analysis in the AEM

The corrections normally associated with the analysis of thick SEM specimens do not apply to thin TEM specimens. Consequently, quantitation may be performed by using a simple ratio technique first developed by Cliff and Lorimer at the University of Manchester Institute of Science and Technology (UMIST) in the early 1970's. Cliff and Lorimer observed that matrix corrections are not needed when analyzing very thin films because self-absorption in the film is negligible. In this case, peak intensities are proportional to concentration and specimen thickness. They removed the effects of variable specimen thickness by taking ratios of intensities for elemental peaks and introduced a "k-factor" to relate the intensity ratio to concentration ratio:

$$\mathbf{C_A/C_B = K_{AB}.I_A/I_B}$$

Where I_A peak intensity for element A, and C_A = concentration in weight % or mass fraction. Each pair of elements requires a different k-factor, which depends on detector efficiency, ionization cross-section and fluorescence yield of the two elements concerned. An individual k-factor relates the concentration of two elements to their X-ray peak intensities. Where more than two elements are to be analysed, a number of k-factors may be derived by using external standards to relate known concentrations with measured intensities. If all ratios are taken with respect to a single element (this is called the ratio standard element), an efficiency response curve may be drawn for any given detector/ microscope analytical system (see Figure 8).

Theoretical k-factor values may be determined using the X-ray line type (K series, L series, etc) for the ratio standard you select. For a given X-ray line, A, and ratio standard line, R, the k factor k_{AR} is calculated as follows:

$$\mathbf{k_{AR} = A_A\, w_R\, Q_R\, a_R\, e_R \,/\, A_R\, w_A\, Q_A\, a_A\, e_A}$$

where **A** = atomic weight; **w** = fluorescent yield; **Q** = ionisation cross section; **a** = the fraction of the total line, e.g. $K\alpha / (K\alpha + K\beta)$ for a $K\alpha$ line, and **e** = the detector efficiency at that line energy. When k factors are known relative to the ratio standard, any other k factors can be calculated using the formula:-

$$\mathbf{k_{AB} = k_{AR} \,/\, k_{BR}}$$

Any element can be selected as the ratio standard element (R) if theoretically derived k factors are employed. Conventionally, Si is selected, but other elements such as Fe may be used instead. This selection usually depends upon the type of sample that is commonly analyzed in the microscope.

K factors may also be derived experimentally. A variety of standards have been used to generate these curves and it is important that the composition of the materials used is accurately known, that they are insensitive to the electron beam, and thin enough to conform to the requirements of thin-film analysis. It is also necessary to make a number of measurements per standard to take into account sample inhomogeneity and statistical variation in counts. Note that empirically derived k-factors are system specific in the sense that they are derived for specific beam energy and EDS window thickness. Also, both theoretically and empirically derived k-factors are kV dependent.

If samples exceed ~ 100 nm in thickness, it is necessary to apply density and thickness corrections due to absorption effects.

Correcting for sum peaks

In certain circumstances, count rates may be so high that pulse pile-up occurs. This is due to two or more X-ray photons being counted simultaneously and a resultant peak occurring as a sum peak. For instance, if two Si Kα X-ray are counted at the same time, a peak is generated at 3.48 keV, twice the value of 1.74 Kev normally attributed to Si Kα. Correction software is incorporated into Oxford Instruments' software (**INCA** and **AZtec**) to correct for this artifact. Not only is the sum peak removed but the counts are reapportioned back to the Si Kα peak so that quant results are not affected. It is important that these sum peaks are detected and dealt with because not only will the quant be affected but these peaks may be wrongly identified and ascribed to another element.

7. Fast Mapping and Linescans with SDDs

Scanning Transmission Electron Microscopes (STEM) can raster the beam over a sample to create a variety of transmitted electron images, including bright-field and dark-field images as well as X-ray maps and linescans. Due to the advent of large-area SDDs, it is possible to collect X-ray maps and linescans over much shorter times than using conventional Si(Li) detectors. In addition, field-emission STEMs with aberration-corrected condenser lenses can create very small probes with extremely high beam currents, which can facilitate X-ray mapping in very short amounts of time, and also allows enough signal to be generated to collect maps from very small structures.

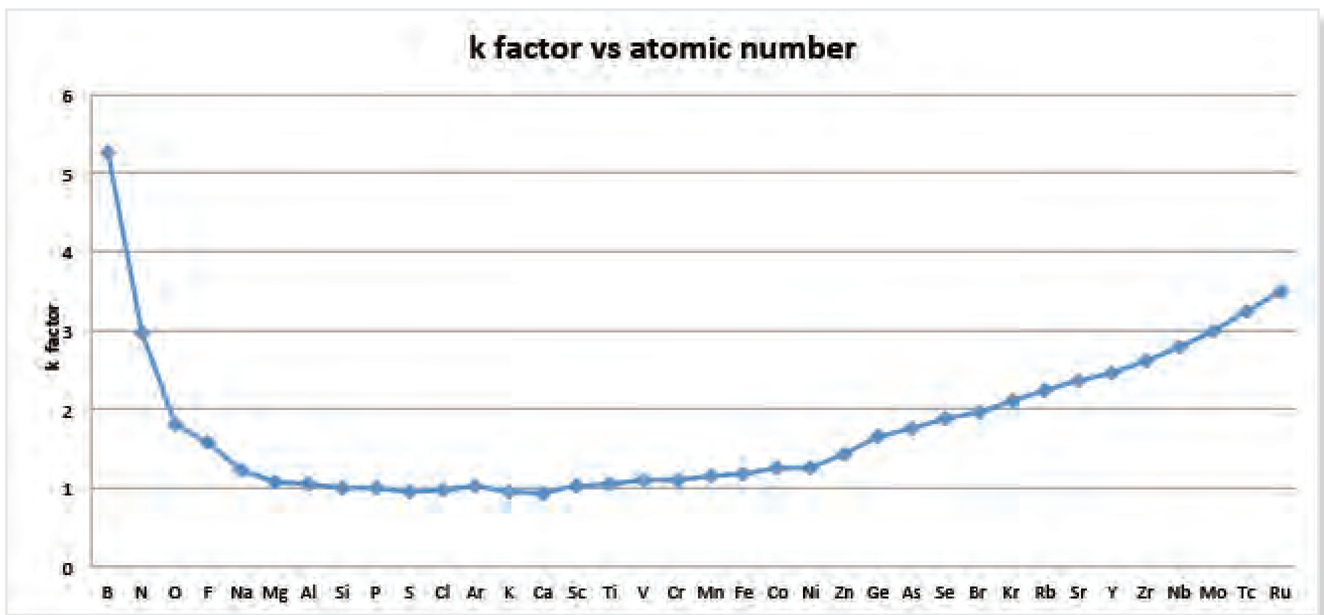

Fig. 8. *Efficiency curve for an SDD detector with window.*

Figure 9 shows an image of a layered photonics structure consisting of alternating layers of Ge, GaAs, Al In P and InP. The X-ray maps show layers as thin as 25 nm. These data were collected on a 200 kV FESTEM. Even the smallest layers were readily discernable in only 5 minutes.

Fig. 9a. Bright field STEM image of layered photonics structure.

FLS mapping and linescans

Very often, there is overlap between elemental peaks. Deconvolution of these peaks is essential for quantitative analysis and accurate peak autoID. However, up until recently, although spectral maps and linescans were collected on a pixel-by-pixel basis with a spectrum at each pixel stored, it was not possible to perform deconvolution and remove background in real time.

New multicore microprocessors now allow for very fast processing of data, and when combined with highly developed software, and 64 bit processing, the software can deconvolute peaks and remove background in real time. This is very important in many cases where overlap occurs because misidentification is a common problem.

In the example below, (Figure 10), we can see spectral maps and a sum spectrum of a semiconductor cross-section. There is an obvious overlap of Si and W, and there is an apparent overlap of P with a minor W peak.

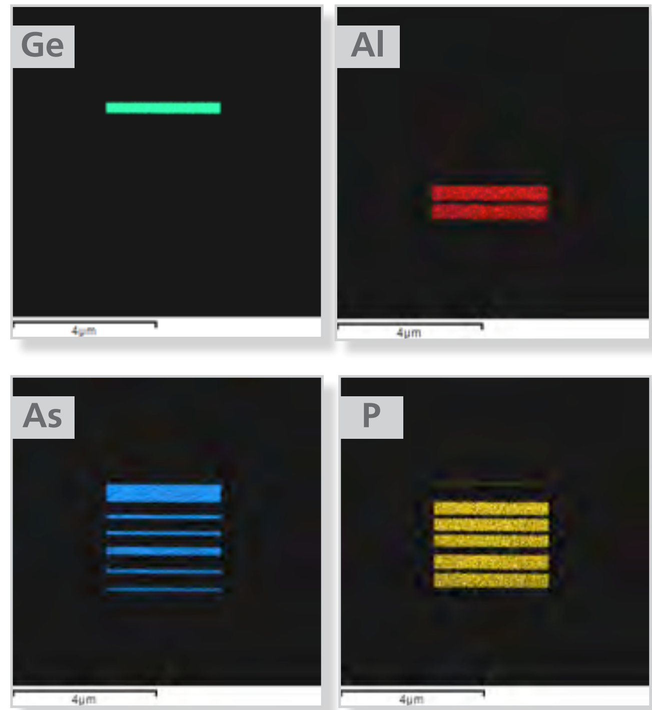

***Fig.** 9b, c, d, e, showing distribution of elements in layered photonics materials. 5 minute map showing layers as small as 25 nm.*

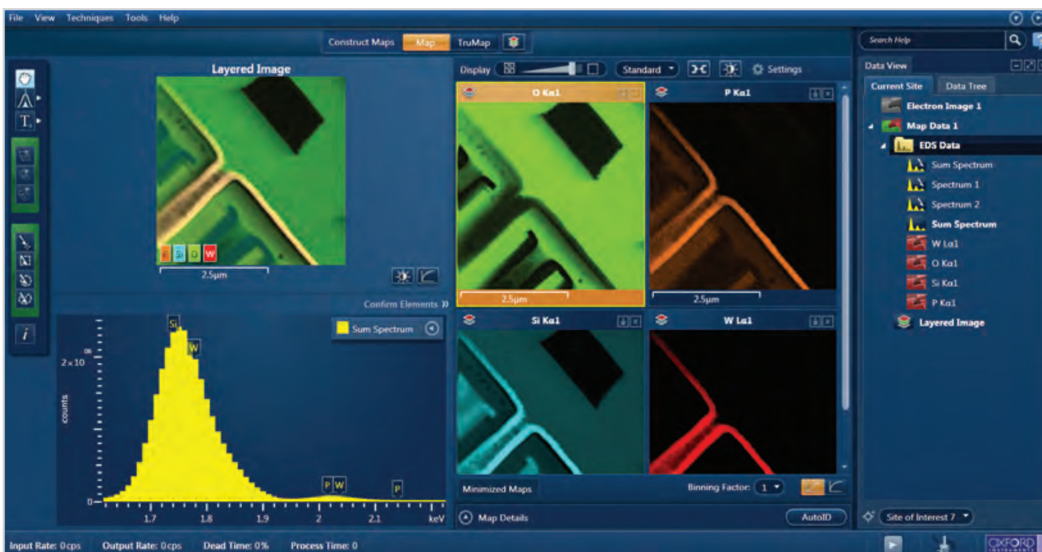

***Fig. 10.** SmartMap of semiconductor showing elemental overlaps.*

It can be seen that in the spectral map, the P and Si follow the W. However, if we then use TruMap (Figure 11), we can now see a totally different distribution because peak deconvolution and background removal have been applied.

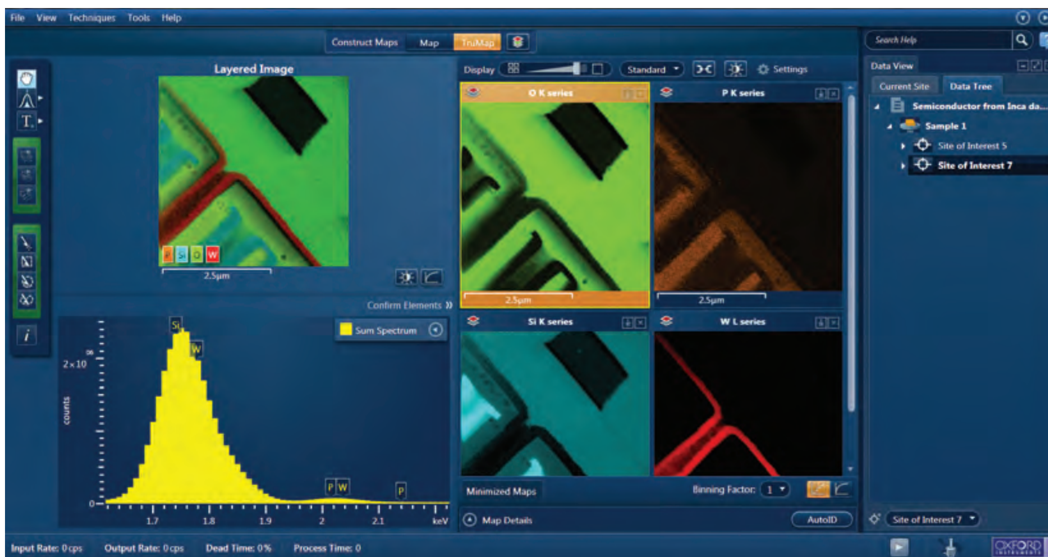

The P and Si no longer follow the W because of the deconvolution of peaks, and the maps are easier to interpret with the background removed. To be able to apply these corrections in real time is very beneficial because much time is saved in post-processing of data.

Fig. 11. *Peak deconvoluted and background subtracted X-ray maps (TruMaps) of semiconductor device.*

AutoLock Drift Correction

At very high magnifications, especially under high beam currents, samples tend to drift even if the proper precautions are applied - i.e. letting the TEM and sample holder adjust for environmental conditions when transferring the specimen from the outside environment to inside the microscope column. AutoLock corrects this drift so that X-ray maps are not blurred and features may clearly be seen. This is especially important if atomic column mapping is attempted because sample drift destroys any meaningful data.

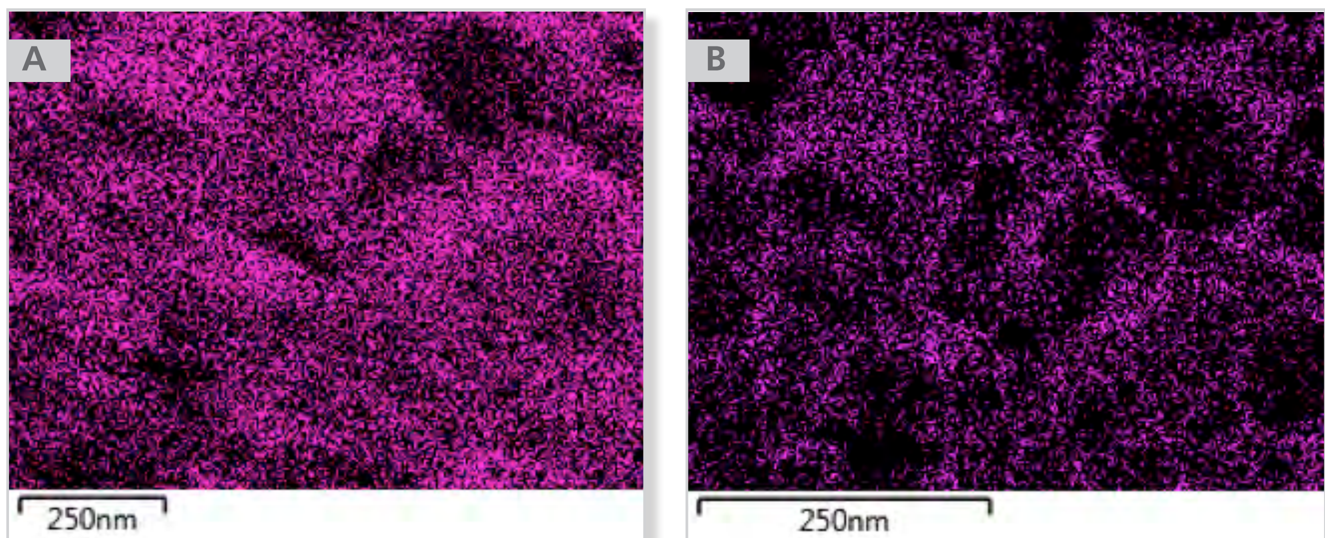

Fig.12. *The two X-ray maps are of the same area, a) is without AutoLock and b) is with AutoLock.*

As can be seen from the above maps, (Fig. 12) AutoLock makes a large difference by stabilizing the image so that individual features can be observed.

Conclusions

TEM remains a formidable tool for the analysis of materials down to the atomic scale. With the advent of aberration correctors and high-brightness field-emission guns, analysis with ultra fine probes can be formed with very high beam-current density. A modern EDS system should be able to handle both high counts (100 kcps) and have a large solid angle to accommodate TEMs and samples that generate very low X-ray emission. It is now possible to create X-ray maps in minutes rather than hours as was the case before the advent of SDDs. Modern, easy to use software offers important features, such as drift correction (AutoLock in **AZtec**TEM) and peak deconvoluted /background subtracted X-ray mapping (TruMap in **AZtec**TEM).

Suggestions for further reading:-

Cliff,G. and Lorimer, G.W. (1975) The Quantitative Analysis of Thin Specimens. J. Microsc. 103:179.

Garratt-Reed, A.J. and Bell, D.C. (2003) Energy Dispersive Analysis in the Electron Microscope. Royal Microscopical Society Series-49, Bios Scientific Publishers Ltd.

Oxford Instruments. (2012) Silicon Drift Detectors Explained. Oxford Instruments Analytical Ltd.

Williams, D.B. and Carter, C.B. (2009) Transmission Electron Microscopy, a Textbook for Materials Science, Springer, New York.

Wood, J.E., Williams, D.B. and Goldstein, J.I. (1984) Experimental and theoretical Determination of k Factors for Quantitative X-ray Microanalysis in the Analytical Electron Microscope. J. Microsc. 133:255.

Please visit **www.oxford-instruments.com/nanoanalysis**

This publication is the copyright of Oxford Instruments plc and provides outline information only, which (unless agreed by the company in writing) may not be used, applied or reproduced for any purpose or form part of any order or contract or regarded as the representation relating to the products or services concerned. Oxford Instruments' policy is one of continued improvement. The company reserves the right to alter, without notice the specification, design or conditions of supply of any product or service. Oxford Instruments acknowledges all trademarks and registrations. © Oxford Instruments plc, 2013. All rights reserved. Document reference OINA/TEMExplained/0813.

The Business of Science®